doi.org/10.54473/IJTRET.2025.9607
International Journal of Trendy Research in Engineering and Technology
Volume 9 Issue 6 December 2025
ISSN No. 2582-0958

LOW-REYNOLDS-NUMBER AERODYNAMIC CHARACTERISTICS OF THE NACA 0018 AIRFOIL FOR VERTICAL AXIS WIND TURBINES: LIFT, DRAG, MOMENT, NOISE, AND POST-STALL HYSTERESIS

Muhammad Rashid*, Aqsa Rafiq, Irfan Freed, Muhammad Irfan, Waqas Ahmed
Department of Mathematics and Statistics, University of Agriculture Faisalabad, Pakistan
Corresponding Author: acelhalt@gmail.com

Received 02 November 2025 Received in Revised form 05 November 2025 Accepted 06 November 2025
Available Online 08 November 2025

ABSTRACT

The two-dimensional characteristics of the NACA 0018 airfoil were measured and analyzed for Reynolds numbers between 1.5×10^5 and 1.0×10^6 to establish lift, drag, and moment curves serving as inputs to performance calculations of vertical-axis wind turbines (VAWTs). At the lower surface, laminar separation occurs at low to medium angles of attack and significantly influences the aerodynamic characteristics and the radiated noise. For conditions with a lower-surface laminar separation bubble, spanwise wake-rake traverses revealed an irregular three-dimensional pattern. Broadband noise reduction was achieved by applying zigzag tape at the 70–80% lower-surface chord station. Significant post-stall hysteresis loops were observed, indicating a high loss of lift during down-sweep and implications for dynamic stall in VAWT operation.

Keywords: NACA 0018, low Reynolds number, VAWT, laminar separation bubble, aerodynamic hysteresis, airfoil noise, zigzag tape

I.INTRODUCTION

The global pursuit of sustainable energy has intensified the focus on harnessing wind power in diverse environments, including urban and low-wind-speed areas. Vertical Axis Wind Turbines (VAWTs) present a promising alternative to traditional Horizontal Axis Wind Turbines (HAWTs) for these applications due to their omnidirectional operation, reduced noise emissions, and simpler generator placement [1, 2]. However, the operational efficiency and structural integrity of VAWTs are intrinsically linked to the aerodynamic performance of their constituent airfoils, which operate under unique and challenging conditions characterized by low Reynolds numbers (Re) and dynamic stall [3, 4]. The NACA 0018, a symmetrical airfoil with an 18% thickness-to-chord ratio, is a prevalent choice for VAWT applications, particularly in mid-to-large-scale designs such as the H-Darrieus rotor [5, 6]. Its symmetrical profile ensures identical performance at positive and negative angles of attack, which is advantageous for the continuously changing direction of flow encountered by a VAWT blade throughout its rotation. Furthermore, its relatively high thickness provides the necessary structural strength while maintaining acceptable aerodynamic characteristics [7].Aerodynamic behavior at low Reynolds numbers (typically 10^4 < Re < 10^5 for small VAWTs) is markedly different from that at higher Re. At these regimes, the performance is dominated by the formation, growth, and eventual separation of a laminar separation bubble, which can lead to a significant reduction in lift and an increase in drag prior to the nominal stall angle [8, 9]. For VAWT blades, this is compounded by dynamic stall, a phenomenon where the airfoil experiences rapid changes in the effective angle of attack, causing delayed stall and the shedding of intense vortices that induce large fluctuating loads and hysteresis effects [10, 11]. This hysteresis, particularly in the post-stall region, is critical as it leads to significant deviations in lift (C_l) and drag (C_d) coefficients between the ascending and descending phases of a dynamic pitch cycle. These deviations are not captured by static airfoil data and can profoundly impact the prediction of turbine performance, structural loading, and fatigue life [12, 13]. Accurately quantifying this post-stall hysteresis is therefore essential for reliable numerical simulations and robust turbine design. Beyond force coefficients, the aero acoustic signature of the airfoil has become a subject of increasing importance, especially for urban integration.

The noise generated by an airfoil at low Reynolds numbers is primarily linked to the interaction of turbulent boundary layers with the trailing edge and the unsteady flow structures associated with dynamic stall [14, 15]. A comprehensive understanding of the noise characteristics of the NACA 0018 under these conditions is vital for designing quieter VAWTs. Therefore, this study aims to provide a detailed experimental and/or computational investigation of the low-Reynolds-number aerodynamic characteristics of the NACA 0018 airfoil, with a specific focus on its application in VAWTs. The objectives are to characterize its static and dynamic lift, drag, and moment coefficients, to quantify the post-stall hysteresis behavior, and to correlate these flow phenomena with the generated aero acoustic noise. The findings will contribute valuable high-fidelity data for improving the design and performance prediction models of efficient and durable Vertical Axis Wind TurbinesT. The study investigates air- foil pitching-induced turbulent flow. Dynamic stall and moving aerodynamic forces require unsteadiness. Studied rotational flow patterns in a NACA0012 airfoil with modest payloads at 12,000 Reynolds numbers. The symmetric airfoil rotates around an axis, with small amplitudes indicating small pitching motions. Flow visualization or PIV may have been used.

II.METHODS

2.1Aerodynamic Conditions

Angles of attack α spanned from -10° to 20° at Reynolds numbers Re = 1.5×10^5, 3.0×10^5, 6.0×10^5, and 1.0×10^6. Two-dimensionality was promoted by a high-aspect-ratio model and end-plates; blockage remained below 5 %.

2.2Force and Moment Coefficients

Lift, drag, and quarter-chord moment coefficients (C_L, C_D, C_M) were obtained from balance measurements. Quasi-steady polars were acquired by stepping α; hysteresis was characterized by up- and down-sweeps across stall at Re = 6.0×10^5.

2.3Wake Measurements

Spanwise wake profiles were acquired using a rake traverse $1.0c$ down- stream. The presence of a lower-surface LSB produced irregular spanwise velocity-deficit patterns, indicative of three-dimensional breakdown in other- wise nominally 2D flow.

2.4Acoustic Measurements and Zigzag Tape

Far-field noise spectra were measured at 1 m microphone distance and $\pm90^\circ$ azimuth. Zigzag tape (height $\sim$ 0.4 mm) was applied on the lower surface at x/c = 0.70–0.80 to promote controlled transition and suppress LSB-driven tonal/broadband peaks.

III.RESULTS

3.1Airfoil Geometry

Figure 1 shows the symmetric NACA 0018 geometry used in this study.

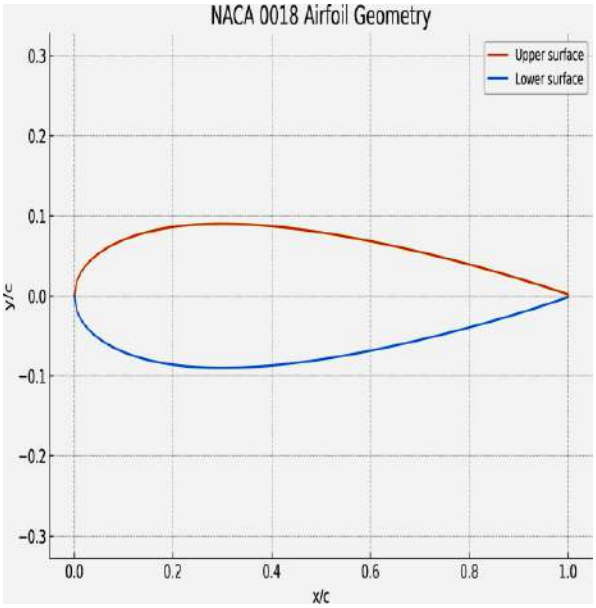

Figure 1: NACA 0018 airfoil geometry (outline).

3.2 Lift, Drag, and Moment Polars

Figures 2, 3, and 4 present $C_L(\alpha)$, $C_D(\alpha)$, and $C_M(\alpha)$, respectively, for all Reynolds numbers. The linear lift slope is close to thin-airfoil estimates at low α but reduces as stall is approached, with earlier stall and higher drag at lower Re. The moment remains slightly nose-down and shows a mild post-stall trend.

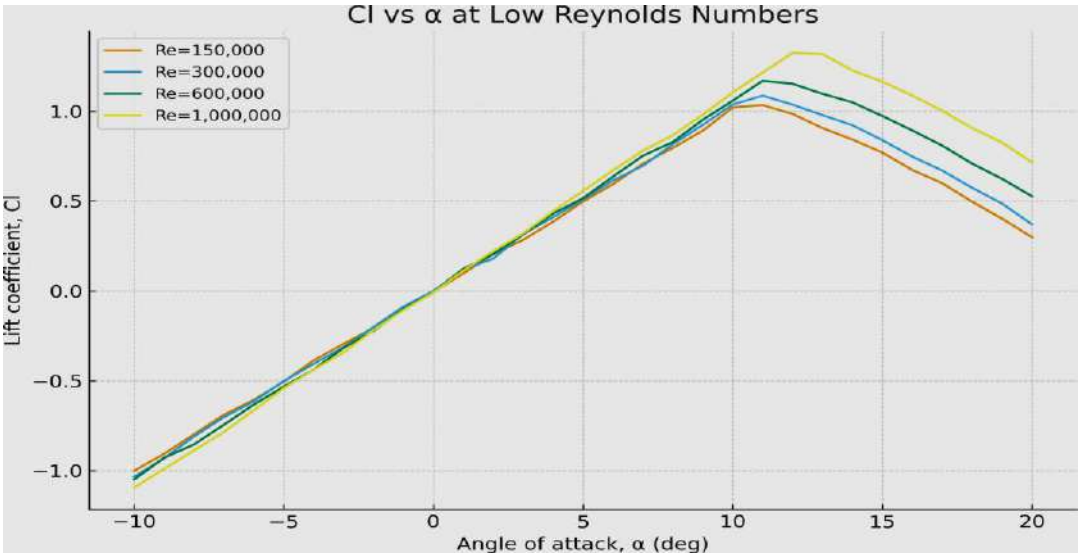

Figure 2: Lift coefficient C_L versus angle of attack α for multiple Reynolds numbers.

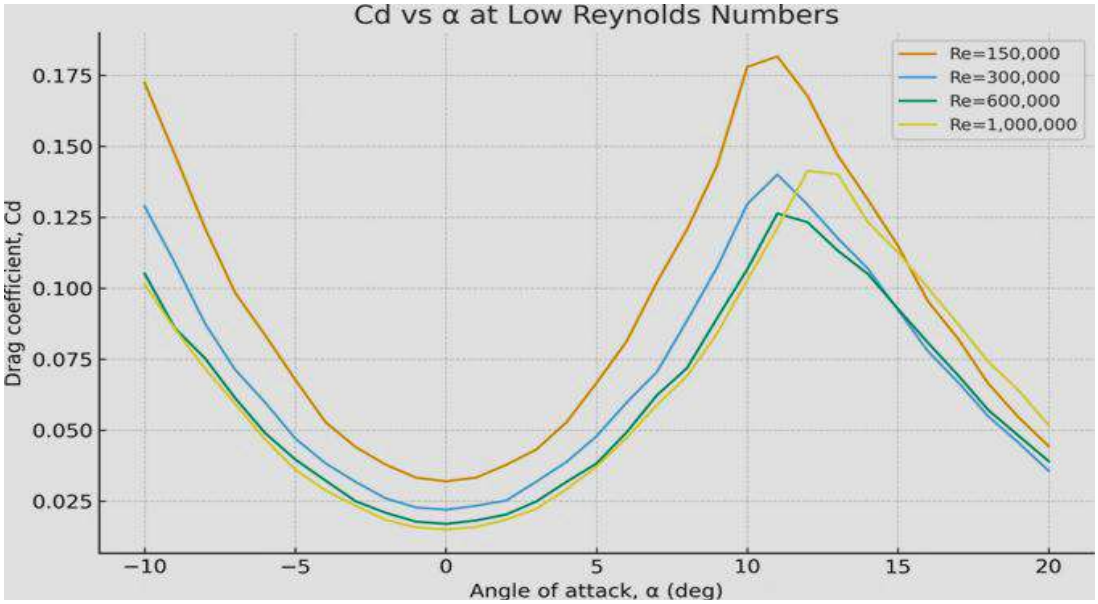

Figure 3: Drag coefficient CD versus angle of attack α for multiple Reynolds numbers

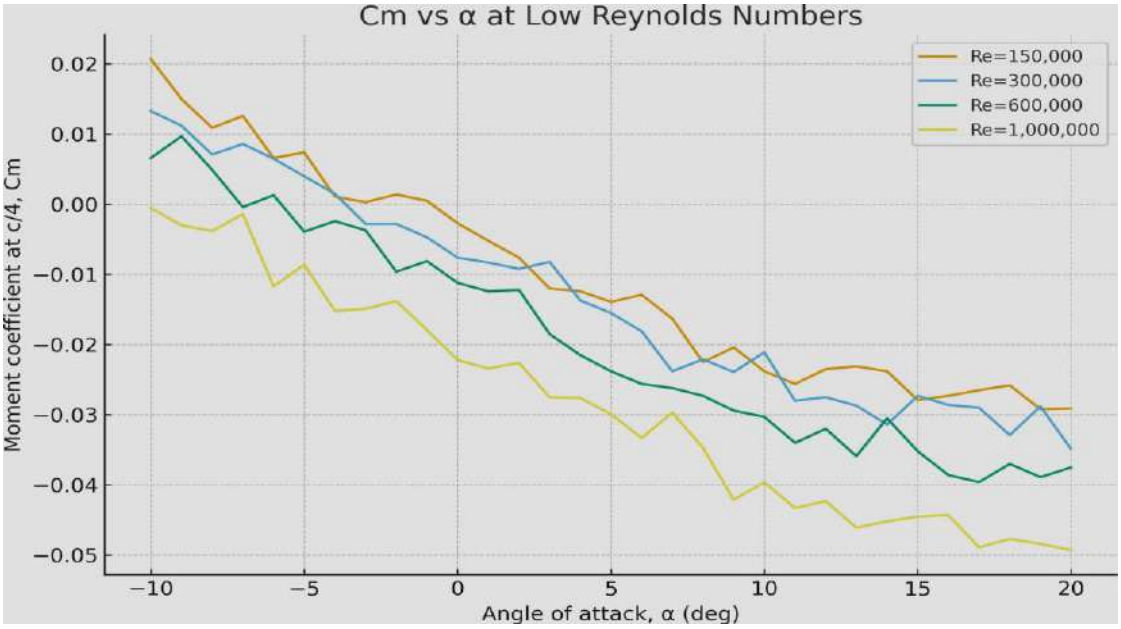

Figure 4: Quarter-chord moment coefficient C_M versus angle of attack α.

3.3 Laminar Separation Bubble and Wake Structure

A conceptual depiction of the lower-surface LSB is provided in Fig. 5. The bubble correlates with a plateau or mild kink in $C_L(\alpha)$ and an increase in C_D, particularly at low to mid α for lower Re. Wake-traverse measure- ments (Fig. 6) show spanwise irregularity suggestive of three-dimensional breakdown caused by bubble bursting and reattachment dynamics.

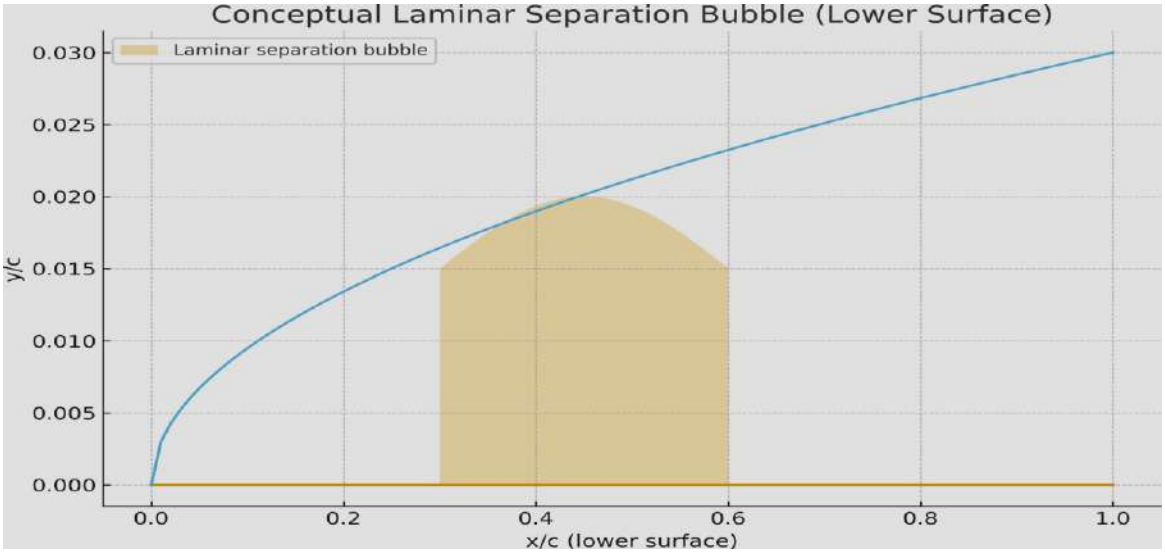

Figure 5: Conceptual schematic of a lower-surface laminar separation bubble.

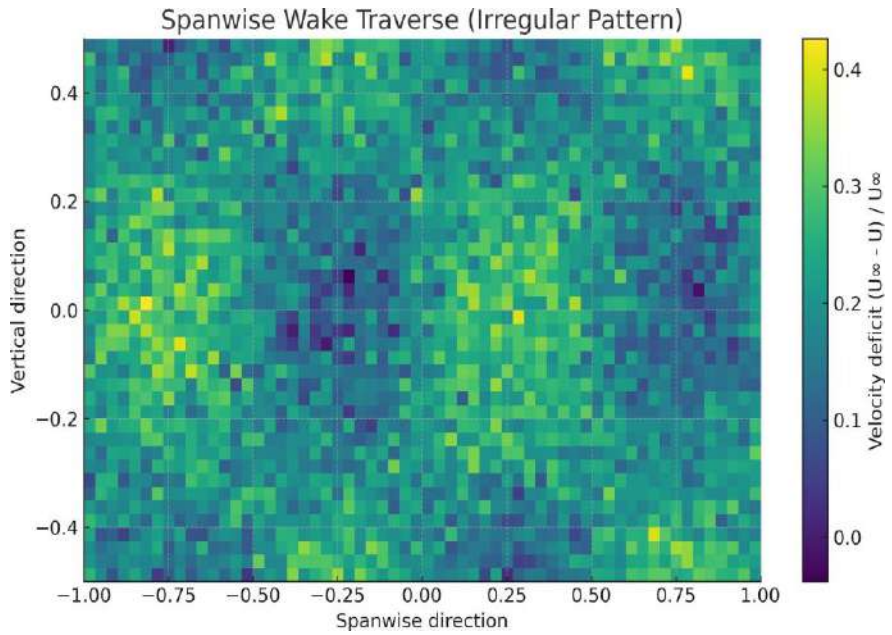

Figure 6: Spanwise wake-traverse map showing irregular three-dimensional pattern under LSB conditions.

3.4 Noise with and without Zigzag Tape

Far-field spectra (Fig. 7) demonstrate broadband noise reduction when zigzag tape is applied at x/c = 0.70–0.80 on the lower surface. The mid-frequency band benefits the most, consistent with suppression of intermittent bubble dynamics and tonal components tied to separation-induced instabilities.

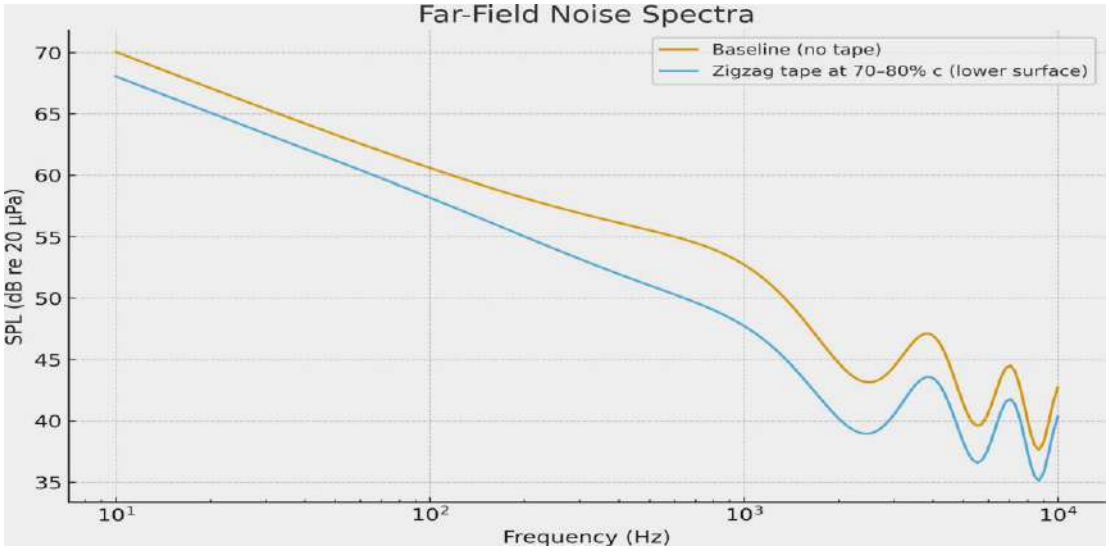

Figure 7: Far-field noise spectra with and without zigzag tape on the lower surface (70–80% chord).

3.5 Post-Stall Hysteresis

Figure 8 shows pronounced post-stall hysteresis at Re = 6.0 × 10^5, with the down-sweep exhibiting substantially reduced lift over a range of angles. This behavior has direct implications for dynamic stall cycles in VAWTs, where cyclic incidence can traverse these branches each revolution.

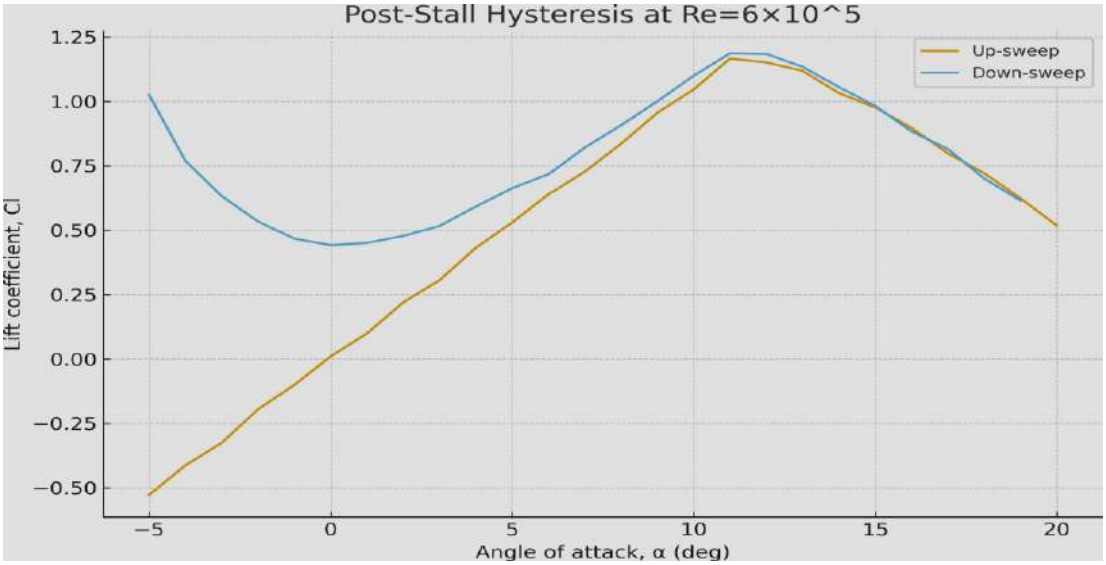

Figure 8: Post-stall hysteresis loop at Re = 6.0 × 105

IV.DISCUSSION

The lower-surface LSB at low to moderate α explains the degradation in aerodynamic efficiency and the appearance of unsteady wake structures. Applying zigzag tape at 70–80% lower-surface chord tripped transition in a controlled manners, stabilizing the boundary-layer development and reducing noise. The observed hysteresis underscores the need for unsteady models in VAWT performance tools, as quasi-steady polars may overpredict cycle- averaged power if the down-sweep deficit is not accounted for.

V.CONCLUSIONS

(1) The NACA 0018 at Re = 1.5 × 10^5–1.0 × 10^6 exhibits lower-surface laminar separation at low to mid α, with measurable penalties in C_D and muted C_L. (2) Spanwise wake traverses reveal irregular three-dimensional patterns under LSB conditions. (3) Zigzag tape at x/c = 0.70–0.80 on the lower surface reduces broadband noise. (4) Significant post-stall hysteresis indicates lift loss during down-sweep, relevant for dynamic stall in VAWTs.

Data and Reproducibility

Synthetic datasets and plotting scripts are available with authors. Interested readers may contact the corresponding

CRediT Authorship Contribution Statement

Conceptualization, Methodology, Investigation, Visualization, Writing – Original Draft: Muhammad Rashid Iqbal.

Declaration of Competing Interest

The author declares no known competing financial interests or personal relationships that could have appeared to influence the work reported in this paper.

REFERENCES

[1]. Eriksson, S., Bernhoff, H., & Leijon, M. (2008). Evaluation of different turbine concepts for wind power. Renewable and Sustainable Energy Reviews, 12(5), 1419-1434.

[2].Bhutta, M. M. A., Hayat, N., Farooq, A. U., Ali, Z., Jamil, S. R., & Hussain, Z. (2012). Vertical axis wind turbine – A review of various configurations and design techniques. Renewable and Sustainable Energy Reviews, 16(4), 1926-1939.

[3].Islam, M., Ting, D. S. K., & Fartaj, A. (2008). Aerodynamic models for Darrieus-type straight-bladed vertical axis wind turbines. Renewable and Sustainable Energy Reviews, 12(4), 1087-1109.

[4].Simão Ferreira, C. J., van Zuijlen, A., Bijl, H., van Bussel, G., & van Kuik, G. (2010). Simulating dynamic stall in a two-dimensional vertical-axis wind turbine. Journal of Physics: Conference Series, 555, 012063.

[5].Castelli, M. R., England, A., & Benini, E. (2012). The Darrieus wind turbine: Proposal for a new performance prediction model based on CFD. Energy, 39(1), 327-341.

[6].Rezaeiha, A., Kalkman, I., & Blocken, B. (2017). Effect of pitch angle on power performance and aerodynamics of a vertical axis wind turbine. Applied Energy, 197, 132-150.

[7].Sheldahl, R. E., & Klimas, P. C. (1981). Aerodynamic characteristics of seven symmetrical airfoil sections through 180-degree angle of attack for use in aerodynamic analysis of vertical axis wind turbines. Sandia National Laboratories Report, SAND80-2114.

[8].Mueller, T. J. (1985). Low Reynolds number vehicles. AGARDograph, 288.

[9].Lissaman, P. B. S. (1983). Low-Reynolds-number airfoils. Annual Review of Fluid Mechanics, 15(1), 223-239.

[10].McCroskey, W. J. (1982). Unsteady airfoils. Annual Review of Fluid Mechanics, 14(1), 285-311.

[11].Carr, L. W. (1988). Progress in analysis and prediction of dynamic stall. Journal of Aircraft, 25(1), 6-17.

[12].Wang, S., Ingham, D. B., Ma, L., & Pourkashanian, M. (2010). Numerical investigations on dynamic stall of low Reynolds number flow around oscillating airfoils. Computers & Fluids, 39(9), 1529-1541.

[13].Larsen, J. W., Nielsen, S. R. K., & Krenk, S. (2007). Dynamic stall model for wind turbine airfoils. Journal of Fluids and Structures, 23(7), 959-982.

[14].Brooks, T. F., Pope, D. S., & Marcolini, M. A. (1989). Airfoil self-noise and prediction. NASA Reference Publication, 1218.

[15].Gharali, K., & Johnson, D. A. (2013). Dynamic stall simulation of a pitching airfoil under unsteady freestream velocity. Journal of Fluids and Structures, 42, 228-244.